Proceedings for the 13th International Winds Workshop
27 June - 1 July 2016, Monterey, California, USA

OVERVIEW OF SATELLITE-DERIVED WINDS IN NAVGEM

Patricia Pauley[1], Randal Pauley[2], Nancy Baker[1], and Rebecca Stone[3]

[1]Naval Research Laboratory, 7 Grace Hopper Ave, Monterey, California 93943-5502
[2]Fleet Numerical Meteorology and Oceanography Center, Monterey, California
[3]SAIC, Naval Research Laboratory, Monterey, California

Abstract

This paper describes the satellite-derived wind datasets used in NAVGEM (NAVy Global Environmental Model), the U.S. Navy's operational global numerical weather prediction model, as well as the procedures used to superob the data and their impact on forecasts.

SATELLITE-DERIVED WINDS

The satellite-derived wind ("satwind") datasets used operationally in NAVGEM (as of the writing of this paper) are summarized in Table 1.

Data Type	Sensor and/or Satellite	Production Center	Observation Errors
Geostationary AMVs	GOES-13	NESDIS and CIMSS	2.8 – 5.2 m/s
	GOES-15	NESDIS and CIMSS	" "
	Meteosat-7	EUMETSAT and CIMSS	" "
	Meteosat-10	EUMETSAT and CIMSS	" "
	Meteosat-9	EUMETSAT	" "
	Himawari-8	JMA and CIMSS	" "
Polar AMVs	MODIS/Aqua and Terra	NESDIS and CIMSS	2.8 – 5.8 m/s
	AVHRR/MetOp A, B; NOAA 15, 18, 19	NESDIS and CIMSS	3.4 – 5.8 m/s
	VIIRS/NPP	NESDIS and CIMSS	" "
	LeoGeo (composite imagery)	CIMSS	" "
	Global AVHRR (MetOp A, B)	EUMETSAT	" "
Surface winds	WindSat wind vectors	FNMOC	2.8 m/s
	ASCAT wind vectors	KNMI	"
	RapidScat wind vectors	KNMI	"
	SSMIS wind speeds	FNMOC	3.0 m/s

Table 1: **Satellite-derived wind datasets assimilated operationally in NAVGEM with their assigned observation errors. The winds are presented in three categories—Atmospheric Motion Vectors (AMVs) from geostationary satellites, AMVs from polar-orbiters (or composite imagery in the case of LeoGeo winds), and satellite-derived surface winds.**

The U.S. Navy's system is unique in that it uses two datasets for each of the major geostationary satellites—one produced by the operational production centers (NESDIS, EUMETSAT, and JMA) and one produced by CIMSS (University of Wisconsin). Superobs from CIMSS data are offset by half a "prism" (averaging volume) in both latitude and longitude compared to the superobs from data from the operational centers. Polar AMVs are processed similarly, with separate superobs formed for NESDIS and CIMSS datasets where both are available. Note that no distinction is made at present between single-METOP, dual-METOP, and METOP triplet winds in the Global AVHRR data. Sample data coverage diagrams were shown at the workshop and can be found in the PowerPoint from the talk available on the conference web site at http://cimss.ssec.wisc.edu/iwwg/iww13/talks/02_Tuesday/1320_IWW13_NAVGEM_Pauley.pdf.

QC AND SUPEROB PROCEDURES

The satwind processing begins with reading the data, converting direction and speed to u and v wind components, and assigning observation errors that are a function of pressure level for geostationary and polar AMVs and are constant for surface winds (Table 1). Following that, a number of quality control (QC) checks are applied to the data as described in Table 2. The goal of these checks is to reject individual observations that are either bad or suspicious prior to superobbing.

QC check	Data Rejected	Type of Winds Subjected to Check
Duplicates	Only exact duplicates	All satwinds
Invalid observations	Missing lat, lon, pressure, or time	All satwinds
	Missing background value	All satwinds
Observations with low confidence	QI < provided threshold	EUMETSAT geostationary AMVs
	QI < 50	CIMSS geostationary AMVs
	QI < 60	CIMSS polar AMVs (including LeoGeo)
	RFF < 40	CIMSS geostationary/polar AMVs
	Flagged as low accuracy or possible ice	SSMIS wind speeds
	Flagged as non-ocean	WindSat wind vectors
Vertical limits	Pressure >= 975 hPa	All geostationary/polar AMVs
	Pressure < 175 hPa	Meteosat-10 AMVs
	Pressure < 125 hPa	All other geostationary/polar AMVs
	VIS with pressure < 675 hPa	Geostationary AMVs except Meteosat-10
	Shortwave IR with pressure < 675 hPa	Geostationary AMVs
	IR with 675 hPa > pressure >= 425 hPa	Geostationary AMVs except Meteosat-10
	WV or WV-clear with pressure >= 475 hPa	Geostationary AMVs except Meteosat-10
	WV-cloudy with pressure >= 425 hPa	Geostationary AMVs
	Pressure < 275 hPa	MODIS/AVHRR/VIIRS/LeoGeo AMVs
	Pressure >= 725 hPa	MODIS/AVHRR/VIIRS AMVs
	WV with pressure >= 575 hPa	MODIS AMVs
	S. Hemisphere with pressure >= 574 hPa	MODIS/AVHRR/VIIRS AMVs
Latitude limits	Latitude < -60 deg or latitude > 60 deg	MODIS/AVHRR/VIIRS AMVs
Land Masking	Winds over land rejected for: North America (170°W-18°W, 10°N-65°N), Western Europe (18°W-48°E, 37°N-65°N), Australia (100°E-180°, 10°N-60°S)	All Satwinds except Global AVHRR
	Winds over land rejected for: Greenland (65°W-45°E, 50°N-90°N),	MODIS/AVHRR/VIIRS/LeoGeo AMVs
	IR winds over land rejected for: Antarctica (60°S-90°S)	MODIS/AVHRR/VIIRS/LeoGeo AMVs
Magnitude limits	Speed < 3 m/s	Geostationary/polar AMVs, SSMIS speeds
Innovation (O-B) limits	Vector innovation magnitude < 8 – 12 m/s, as a function of pressure	Geostationary/polar AMVs, surface vectors

Table 2: **Quality control checks applied to satellite-derived wind datasets assimilated operationally in NAVGEM.**

The individual observations that pass QC are binned into “prisms” that have a depth of 50 hPa. The prism “height” is held constant at a specified size in degrees of latitude; the size is set to 2.0° for geostationary and polar AMVs and for SSMIS wind speeds and to 1.5° for surface wind vectors. The prism “width” then varies subject to two constraints. First, the width is set equal to the height for prisms at the equator and is varied with latitude to keep the area approximately constant, and second, the number of prisms in a latitude band is required to be an integer. This means that the number of prisms present in a latitude band decreases moving from the equator toward either pole and that the longitudinal extent of a prism (in degrees) increases at the same time. In addition, CIMSS geostationary winds use prisms that are offset from the prisms for NESDIS/EUMETSAT/JMA geostationary winds by one-half prism in both latitude and longitude. This is done in an effort to keep the superobs from the two datasets from being too close together spatially.

Once the satwinds are binned, then an attempt is made to form superobs. The guiding principle here is that averaging to form superobs is performed only for similar observations, with ‘similar’ defined according to the criteria listed in Table 3. Note that innovation is defined as observation minus background (O-B) and that superobs are normally computed from u and v components even though some of the criteria are phrased in terms of speed and direction.

Superob Criteria
In the same prism and 50 hPa layer
Generated by the same processing center
From the same satellite (or multi-satellite product)
From the same channel
With times within one hour
With at least the minimum number of observations
With speeds (or innovations) within 7-14 m/s depending on speed
With direction (or innovations) within 20° or u and v components (or innovations) within 5 m/s

Table 3: **Criteria used to determine whether a group of observations can be used to form a superob**

The minimum number of observations needed to form a superob varies with satwind type; at least two observations are required for geostationary and polar AMVs, four for SSMIS wind speeds and RapidScat wind vectors, and eight for ASCAT and WindSat wind vectors. Isolated winds are accepted as 'single-ob superobs' only for Meteosat winds produced by CIMSS and AVHRR winds.

If the collection of observations in a prism meets all but one of the last two criteria in Table 3, the observations are examined to see if one or two can be rejected as outliers to allow the remaining observations to meet the criteria and form a superob. If this is unsuccessful, the prism is divided into quarters horizontally, and the observations within each quarter are examined to see if they meet the criteria. Quartering is performed to improve the depiction of the wind field in regions of horizontal shear. An example was shown at the workshop and can be seen in the PowerPoint at the link provided above.

Finally, an adjustment to the magnitude of the u and v superobs is made to preserve kinetic energy. This is done by requiring that the speed of the superob equal the average speed of the individual observations.

ASSIMILATION IN NAVGEM AND OBSERVATION IMPACT

Once superobs are formed, they are presented to NAVGEM for assimilation. The data assimilation system in NAVGEM is NAVDAS-AR, a four-dimensional variational data assimilation system that operates in observation space (Xu et al., 2005); the model in NAVGEM is a semi-Lagrangian semi-implicit spectral global model (Hogan et al., 2014). NAVGEM also includes the calculation of FSOI (Forecast System Observation Impact), which will be the focus of the remainder of this paper. FSOI is computed using the adjoint of the model and is a means of quantifying the contribution of observations to a reduction in the 24-hour forecast error as measured by the moist energy norm (Langland and Baker, 2004).

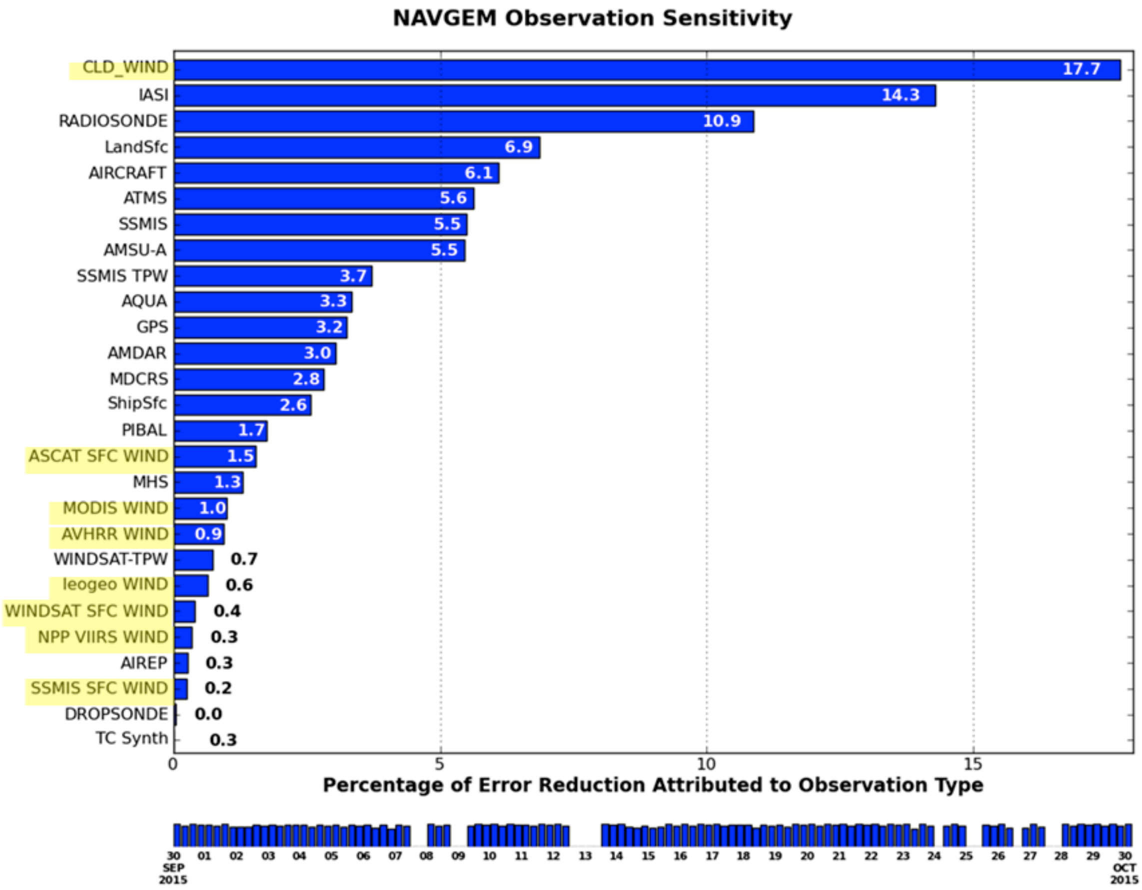

Figure 1: **Percentage of error reduction in 24-hour forecasts for the operational NAVGEM run for October 2015 with data availability shown at the bottom of the graph. Satellite-derived winds are highlighted in yellow.**

Figure 1 shows a typical FSOI bar chart with geostationary winds ("CLD_WIND") providing 17.7% of the error reduction, polar feature-track winds (MODIS, AVHRR, VIIRS, and LeoGeo) providing another 2.8%, and surface satellite winds (ASCAT and WindSat vectors and SSMIS speeds) providing 2.1%. (The percentage of error reduction is determined by dividing the FSOI contribution for individual instrument types by the total FSOI over all instrument types.) This is a greater fractional impact than usually seen at other NWP centers (e.g., Gelaro et al. 2010), although why this should be will not be examined in this paper.

Although FSOI is typically summed over all variables for a particular instrument, values can also be summed over a single variable (or a pair of variables for wind) to get the contributions to the total error reduction for that variable. The remaining figures portray the percentage of error reduction attributable to wind observations (u and v components) from satellite platforms, radiosondes, aircraft, ships, buoys, and surface land stations.

There is considerable variability in FSOI both on a day-to-day basis as well as within one day (Figure 2). Here the FSOI and counts are summed for wind observations for individual six-hour analysis windows for the period Sept 2015-April 2016. Geostationary AMVs (dark blue) are present in the greatest numbers and provide the greatest error reduction as well. Although radiosonde winds (red) are nearly absent at 0600 and 1800 UTC, they provide the second largest error reduction for the analysis windows centered at 0000 and 1200 UTC. Aircraft winds (teal) are available in greater numbers than radiosonde winds but provide less error reduction, most likely a result of the concentration of the aircraft flights (and so redundancy of the data) in and between wealthier countries (e.g., North America, Europe, North Atlantic, East Asia, and Eastern Australia) with relatively few flights over the Pacific, Indian, and Southern Oceans as well as Russia, South America, and Africa. Other satellite wind datasets also provide a significant contribution to error reduction—polar AMVs (yellow), surface satwinds (purple), and global AVHRR AMVs in March and April (cyan). Winds from surface platforms (green) as well as SSMIS speeds (black) have small counts and provide only a small contribution to the error reduction.

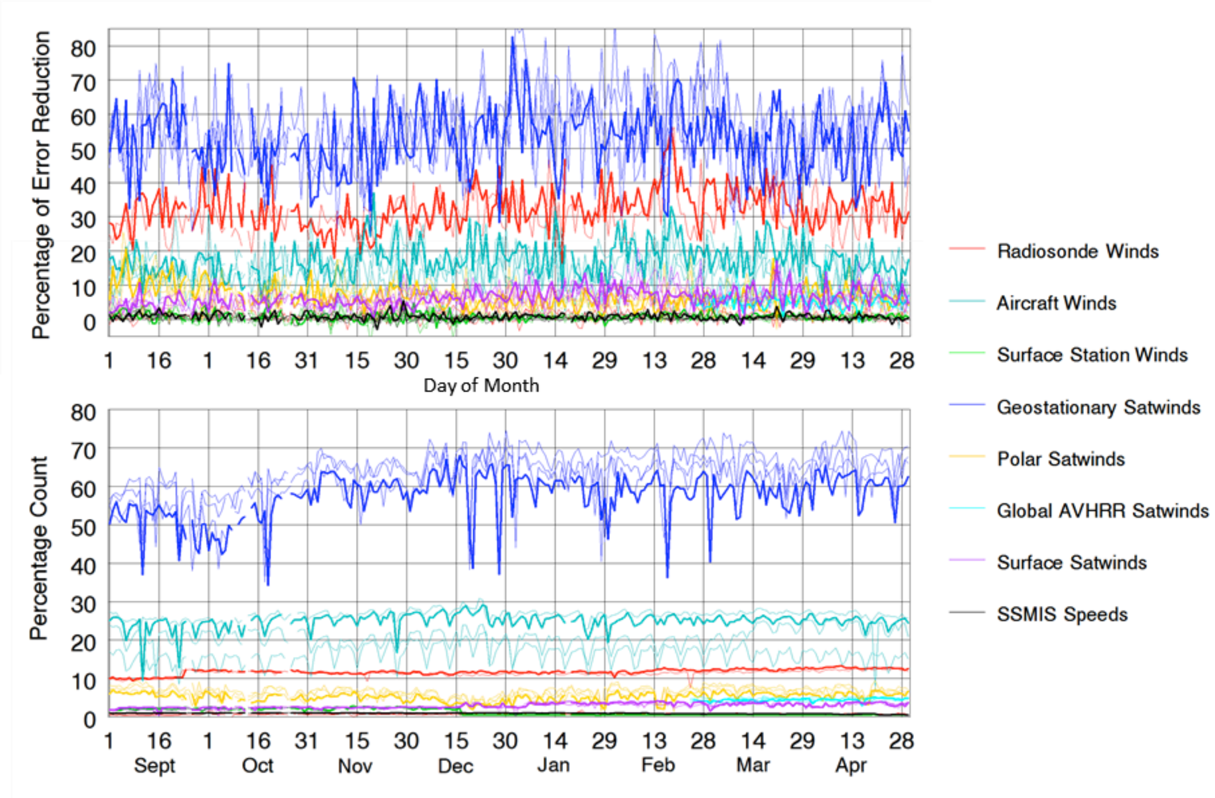

Figure 2: **Percentage of error reduction (top) and percentage count (bottom) for wind observations in 24-hour forecasts for the operational NAVGEM run for September 2015 to April 2016 as a function of time. Bold lines indicate forecasts from 0000 UTC, while thin lines indicate forecasts from 0600, 1200, and 1800 UTC. The percentage error reduction and percentage count were computed relative to the average FSOI (-2.4012 J/kg) and average count (768582) per analysis window for the entire period.**

There were several significant changes in the observations used in NAVGEM during the period portrayed in Fig. 2. BUFR radiosonde data were introduced on 23 September 2015, RapidScat surface wind vectors (included with Surface Satwinds in Fig. 2) on 16 December 2015, and Global AVHRR AMVs on 24 February 2016. In addition, CIMSS switched from MTSAT to Himawari-8 on 4 December 2016. All four changes can be seen in the percentage counts in Fig. 2.

To get a better view of the current behaviour of the NAVGEM system, the percentage error reduction and average counts were computed for just March-April 2016, after all of these changes went in the system (Fig. 3). It is interesting to note that the geostationary satwinds and aircraft winds have a percentage error reduction that is smaller than their percentage count, while the opposite is true for radiosonde winds, surface satwinds, and global AVHRR satwinds. The geostationary satwinds have a disproportionately large contribution at 0600 UTC, when few radiosonde winds are available and aircraft winds are at a minimum. Global AVHRR and surface satwinds also have increased error reduction at 0600 and 1800 UTC when radiosonde data are nearly absent.

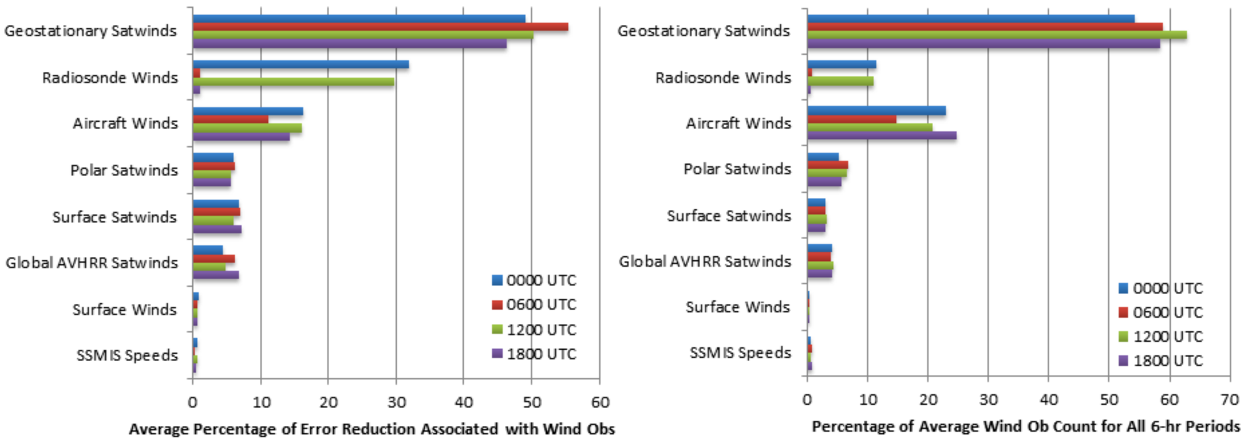

***Figure 3:* Percentage of error reduction (left) and percentage count (right) for wind observations in 24-hour forecasts for the operational NAVGEM run for March-April 2016. Values were computed separately for each six-hour analysis time window centered on the times indicated in the legend.**

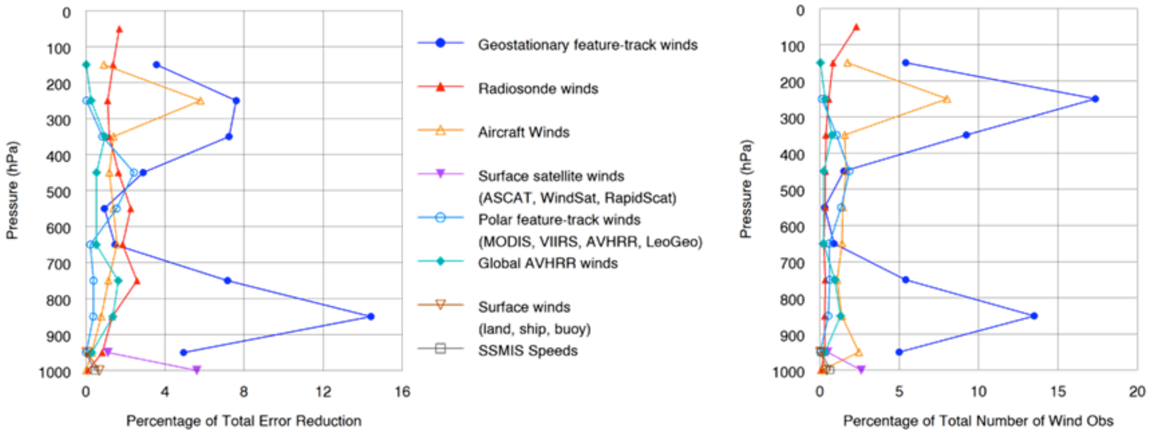

***Figure 3:* Percentage of error reduction (left) and percentage count (right) for wind observations in 24-hour forecasts for the operational NAVGEM run for March-April 2016 binned by pressure.**

Figure 4 shows vertical profiles of the contributions and demonstrates how each of the wind data types provides a unique contribution. Geostationary winds have two peaks in counts, roughly at 850 mb and 250 mb. The lower-tropospheric peak is associated with visible, infrared, and shortwave infrared winds, while the upper-tropospheric peak is associated with infrared and water vapor winds. The percentage error reduction from geostationary winds associated with the upper peak is smaller than that of the lower peak, likely a result of the abundance of aircraft winds in the vicinity of the upper peak. Global AVHRR winds also have a double-peaked distribution with their greatest contribution in the lower troposphere. Radiosonde winds play a significant role in the error reduction at nearly all levels, but are especially important in the mid-troposphere (700-500 hPa) between the two peaks in geostationary winds and above 100 hPa where they are the only source of wind data. Surface satwinds have the largest contribution to error reduction at the lowest levels, where geostationary AMVs are not available. Polar AMVs are important in polar latitudes where geostationary winds are also not available, with their greatest contribution to error reduction at 600-300 hPa.

SUMMARY

This paper provided an overview of the processing used for satellite-derived winds in NAVGEM. NAVGEM uses satwinds from a variety of sources in its operational run, including geostationary AMVs from GOES-13, GOES-15, Meteosat-10, Meteosat-7, and Himawari-8; polar AMVs from MODIS (Aqua and Terra), AVHRR (MetOp A and B, NOAA 15, 18, and 19), VIIRS (NPP), and composite imagery (LeoGeo) as well as global AVHRR AMVs from METOP A and B; surface wind vectors from ASCAT, RapidScat, and WindSat; and surface wind speeds from SSMIS. These winds are averaged to form superobs after QC is applied to the individual observations; NAVGEM then assimilates the superobs.

FSOI statistics demonstrate that geostationary AMVs provide the greatest contribution to percentage error reduction out of all of the types of wind observations assimilated. Polar AMVs, surface satwinds, and global AVHRR AMVs also provide a significant contribution to the error reduction, but less than that provided by radiosonde and aircraft winds.

REFERENCES

Gelaro R, Langland RH, Pellerin S, Todling R (2010) The THORPEX observation impact intercomparison experiment. Monthly Weather Review, **138**, pp 4009-4025.

Hogan TF, Liu M, Ridout JA, Peng MS, Whitcomb TR, Ruston BC, Reynolds CA, Eckermann SD, Moskaitis JR, Baker NL, McCormack JP, Viner KC, McLay JG, Flatau MK, Xu L, Chen C, Chang SW (2014) The navy global environmental model. Oceanography, **27(3)**, pp 116–125.

Langland RH, Baker NL (2004) Estimation of observation impact using the NRL atmospheric variation data assimilation adjoint system. Tellus, **56A**, pp 189-201.

Xu L, Rosmond T, Daley R (2005) Development of NAVDAS-AR: formulation and initial tests of the linear problem. Tellus, **57A**, pp 546–559.